Materials Research. 2015; 18(2): 245-249
DOI: http://dx.doi.org/10.1590/1516-1439.279314

CO_2 Corrosion in the Region Between the Static and Turbulent Flow Regimes

Lilian Raquel Moretto Ferreira[a]*, Haroldo Araujo Ponte[b], Luciana Schmidlin Sanches[b], Ana Carolina Tedeschi Gomes Abrantes[b]

[a]Centro Universitário Tupy – UNISOCIESC, Joinville, SC, Brazil
[b]Laboratório de Eletroquímica de Superfícies e Corrosão, Universidade Federal do Paraná – UFPR, Curitiba, PR, Brazil

Received: March 9, 2014; Revised: March 4, 2015

This paper discusses the influence of the flow of a fluid from the static regime to the turbulent in CO_2 corrosion experienced by low carbon steel. A more comprehensive approach to CO_2 corrosion implies taking the free flowing velocity and shear stress of the fluid and the surface roughness of the material into consideration. Low carbon steel samples in two different superficial finish conditions were used as the rotating cylinder electrode. The corrosion rate were determined by linear polarization at 25 °C in a 0.5 mol/L $NaHCO_3$ solution purged with CO_2 at 1 atm pressure in pH 7.5. The effect of superficial finish on CO_2 corrosion in flow conditions was studied. The results obtained showed that the corrosion rate increases with flow velocity and is influenced by surface roughness.

Keywords: *corrosion under flow, CO_2 corrosion, surface roughness*

1. Introduction

It is known that CO_2 corrosion is the predominant form of corrosion found in the oil and natural gas industry[1]. This is generally because of the crude oil and natural gas from the oil reservoir/gas well usually contains some level of CO_2. The extraction of the oil and gas in deep reservoir, the pre-salt, bring major challenges to industry that besides other peculiarities, presenting a high level of contamination with CO_2. However, the evaluation of the corrosion mechanism is performed in stagnant solutions and so the hydrodynamic factors are ignored.

The intensity and the corrosion mechanism on the internal wall of a pipelines are strongly dependent on surface phenomena which include the interactions of the pipeline wall with the electrolyte flow. There is a wide variety of models for understanding the CO_2 corrosion of carbon steel[2,3,4,5,6,7]. It is known that the CO_2 effect is associated with the increased amount of hydrogen developed in the cathode and with the formation of an iron carbonate film as a corrosion product on the steel surface. Many of the CO_2 corrosion models associated with electrolyte flow are no longer empirical and are described by computational methods[8] .

The currently accepted CO_2 corrosion mechanism involves the hydration of CO_2 and formation of H_2CO_3. The cathodic reaction that describes this process is given by:

$$CO_2 + H_2O \leftrightarrow H_2CO_3 \quad (1)$$

This reaction takes place in a solution as follows:

$$H_2CO_3 \leftrightarrow H^+ + HCO_3^- \quad (2)$$

$$HCO_3^- \leftrightarrow H^+ + CO_3^{2-} \quad (3)$$

*e-mail: lilian@sociesc.org.br

The anodic reaction initially involves iron oxidation on the electrode surface and its dissolution in the following steps:

$$Fe + OH^- \rightarrow FeOH + e^- \quad (4)$$

$$FeOH \rightarrow FeOH^+ + e^- \quad (5)$$

$$FeOH^+ \rightarrow Fe^{2+} + OH^- \quad (6)$$

When the salt solubility is exceeded, the iron carbonate film precipitates on the steel surface.

$$Fe^{2+} + CO_3^{2-} \rightarrow FeCO_3 \quad (7)$$

The aqueous corrosion of carbon steel by CO_2 is an electrochemical process that involves the anodic dissolution of steel and the cathodic hydrogen evolution[9]. The overall reaction is:

$$Fe + CO_2 + H_2O \rightarrow FeCO_3 + H_2 \quad (8)$$

The precipitation process on the steel surface can be control the corrosion processes. Depending on experimental conditions, the $FeCO_3$ forming a unifom layer and the corrosion rate decrease due to the presence of a diffusion barrier for the species involved in the corrosion process and the covering and protection of a portion of the steel surface[10].

The hydrodynamic behavior of the fluid can change the $FeCO_3$ precipitation and the corrosion rate. Since corrosion is a surface phenomenon, the fluid dynamics that defines the electrolyte's interactions with the surface is a determining factor in the corrosion processes. The structure of the hydrodynamic boundary layer changes with the increase in the velocity of the fluid and the roughness of the steel surface[11]. Therefore the study of the changes in the boundary

layer is very important to define the mechanism of the corrosion product formation and its behavior in relation to the moving fluid.

Knowledge of the relationship between flow and CO_2 corrosion has become an emerging need for the oil industry and although more than four decades of research have past, the understanding of CO_2 corrosion remains incomplete. The influence of the fluid shear stress on the laminar to turbulent flow transition is still not well understood.

2. Experimental Procedures

A rotating cylinder electrode and electrochemical techniques were used to evaluate the behavior of low carbon steel with CO_2 corrosion and its correlation with the fluid flow on the metallic surface. The conventional 3-electrode electrochemical cell consisted of a glass body with approximate capacity 100 ml, model RDE0010, EG&G Princeton Applied Research. Besides the reference (saturated calomelane) and auxiliary (spiral platinum) working electrodes, a carbon dioxide (CO_2) bubble was attached to the glass cell. A model PGZ 100 VoltaLab 10 Radiometer Analytical potentiostat controlled by the VoltaMaster 4 software was used to perform the experiment and obtain all the electrochemical measurement data.

The electrolyte used was a deaired 0.5 mol/L sodium bicarbonate ($NaHCO_3$) solution saturated with CO_2 by CO_2 bubble for 30 minutes with pH = 7.5 stabilized at room temperature. Bubbling was performed while preparing the solution for the tests and during the tests to maintain a CO_2-rich atmosphere over the electrolyte. The corrosion rates were measured electrochemically using Linear Polarization Resistence (LPR) technique. The carbon steel working electrode was polarized at ± 20 mV and the scan rate was 0.2 mV/s. The corrosion rate was calculated by using cathodic Tafel slope of 120 mV/dec and anodic Tafel slope of 40 mV/dec.

The working electrodes consisted of AISI 1020 steel cylinders with 12.50 mm external diameter and 8.00 mm height. Before each electrochemical measurement series, a different working electrode was smoothed with a 1200 grain sandpaper to remove any superficial oxides.

To verify the influence of superficial roughness in the corrosion rates, some electrodes were submitted to blasting with stainless steel spherical geometry grit in a ROTOMAC machine with 0.71 mm mesh opening. That way, there are two groups of samples: standard (without blasting) and blasted.

The surface roughness was determined with Confocal Microscopy (LEXT 3D – OLS 4000). The surface characterization was made by Scanning Electron Microscope with Energy Dispersive Spectroscopy (JEOL JSM– 6390LV).

2.1. Hydrodynamic behaviour

The corrosion is a surface phenomenon, in this way the fluid dynamics that defines the electrolyte's interactions with the surface is a determining factor in the corrosion processes. In 1904 Prandtl[12] proposed the concept of boundary layers. He showed that many outflows can be analyzed dividing them into two regions, one close to the pipeline and the other covering the remaining outflow. The narrow region adjacent to a solid border is called the boundary layer, in which the effect of viscosity is important. In the region outside the boundary layer, the effect of viscosity is negligible and the fluid can be considered non-viscous[12].

Since every fluid presents viscosity, experimental observation shows that when a fluid flows parallel to a stationary solid surface (metallic wall) the fluid molecules in contact with the surface adhere to the surface and so its velocity is zero. The adjacent fluid layers experience a braking effect shown by the velocity vector *u* in the boundary layer created on the surface of the moving electrode (see Figure 1). Considering that the fluid as a whole is moving, velocity gradients and shear stresses must be present in the outflow. In turn, these shear stresses affect the fluid's motion and interfere in the iron carbonate layer formation mechanism.

Reynolds number (Re) is a parameter to establish the type of velocity boundary layer that develops on the electrode surface. According to Fox et al.[12], Reynolds number gives an effective measurement of the features of the fluid in the system is question and is given by the equation below:

$$\mathrm{Re} = \frac{du}{\nu} \tag{9}$$

Where:
d = cylinder diameter (m)
u = superficial velocity of the cylinder (m/s)
ν = kinematic viscosity of the fluid (m^2/s)

The transition region between the laminar and the turbulent flows occurs at 2000<Re<2400, where there is formation of Taylor vortices in the space between the electrodes, so operating in the transition regime is not recommended for electrochemical studies. For Re>2400, totally turbulent flow is maintained and mass transportation is substantially increased with increased rotation rate. Thus, for comparative purposes, the rotation rates in this study were established at 400 rpm, 800 rpm and 1200 rpm, because it is known that the geometry of the experimental device allows Re>2400, which characterizes the turbulent flow regime as shown in Figure 2.

According to the works cited by Silverman[13] and to norm ASTM G185[14], it is accepted that the shear stress on the cylinder wall be given by the equation below:

$$\tau = \frac{f}{2}\rho u^2 \tag{10}$$

Where:
ρ = specific mass of the fluid (kg/m^3)
u = superficial velocity of the cylinder (m/s)
f = friction factor (dimensionless)

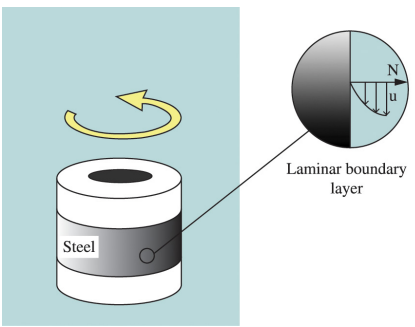

Figure 1. Schematic hydrodynamic boundary layer that develops on the surface of the moving electrode.

The friction factor is mathematically determined by the equation below, considering the experimental measurements before each electrochemical experiment for the average roughness on the cylinder surface. Thus,

$$\frac{f}{2} = o.714(Re)^{-0.39}\left(\frac{d}{\varepsilon}\right)^{-0.2} \quad (11)$$

Where:
Re = Reynolds number (dimensionless)
d = cylinder diameter (m)
ε = superficial roughness (m) obtained from the Ra parameter

In accordance with the experimental planning, the intention is to change the shear stress of the fluid by varying the roughness ε of the electrode.

3. Results and Discussion

The picture in Figure 3 shows the top view of ferrous carbonate layer formed in the standard sample from stagnant condition, at 25 °C in a 0.5 M $NaHCO_3$ solution purged with CO_2 and pH 7.5. The EDS analysis shows the presence of carbon, oxygen and iron, confirming the presence of $FeCO_3$.

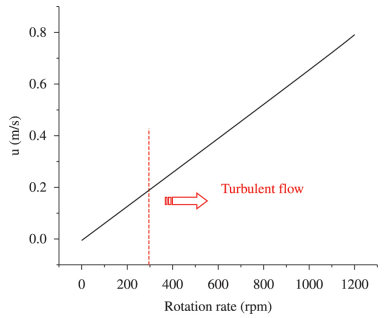

Figure 2. Variation in cylinder tangential velocity as a function of cylinder rotation rate.

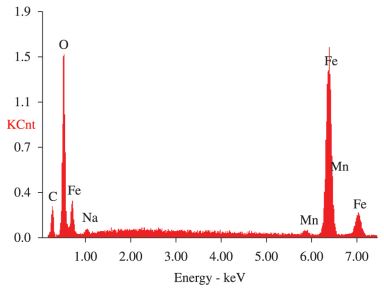

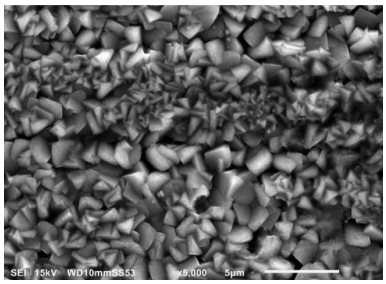

Figure 3. AISI 1020 steel at 25 °C in a 0.5 M $NaHCO_3$ solution purged with CO_2, 1 atm, pH 7.5 and stagnant condition. SEM image of top view with respective EDS analysis.

CO_2 corrosion scale was mainly composed of $FeCO_3$ crystals and became denser, this is due to the crystallization process. The $FeCO_3$ layer, can slow down the corrosion process by being a transport barrier for the corrosive species.

In relation to the corrosion potential of both steel samples, standard and blasted, they did not present significant variation, as shown in Figure 4. This result shows that blasting did not affect the electrochemical behavior of steel.

The roughness parameters shown in Table 1 were obtained with the confocal microscope for the two superficial conditions considered in this study.

The increase in superficial area as a function of blasting was quantified using the ratio between the two superficial area parameters, resulting in a dimensionless area factor F that will be used as the superficial area correlation factor.

$$\text{Area Factor} = F = \frac{A_{blasted}}{A_{standard}} = \frac{3.725mm^2}{1.981mm^2} = 1.880 \quad (12)$$

A typical passivation process behavior was obtained from the anodic polarization of the samples for different rotation conditions, as shown in Figure 5. This shows the polarization curves measured at rotation rates of 0, 400, 800 e 1200 rpm.

It is observed that the corrosion current density (I_{cor}) on polarization curves increases according to the rotation rate until at certain value, after that the corrosion rate density (I_{cor}) decrease. The higher peak value is reached in 800 rpm, at this point the turbulent flow enhances mass transport of species to and away from the steel surface by affecting transport through the boundary layer. For 1200 rpm rotation, there is an inversion of the phenomenon that could be associated with changes in the conditions of the flow on the surface caused by the profile of boundary layer[15]. This behavior is discussed below.

Figure 6 shows the values of CO_2 corrosion rate, expressed as a function of the rotation rate for both superficial finish conditions: standard and increased roughness (blasted).

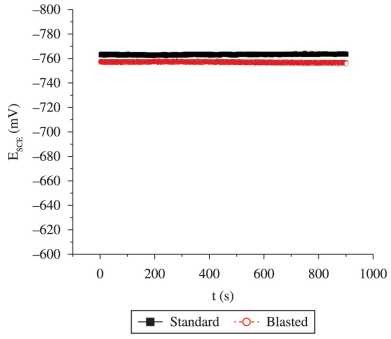

Figure 4. Comparison between the corrosion potential for AISI 1020 steel with standard surface and surface blasted, at 25 °C in a 0.5 M $NaHCO_3$ solution purged with CO_2, 1 atm, pH 7.5 and stagnant condition.

Table 1. Roughness and area measurements.

	R_a (µm)	A (mm^2)
Standard sample	1.076	1.981
Blasted sample	5.160	3.725

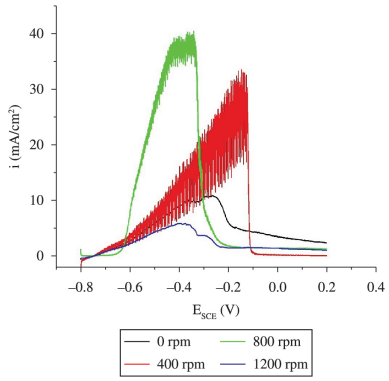

Figure 5. Anodic polarization curves at different rotation rates: 0, 400, 800 and 1200 RPM. of AISI 1020 steel AT 25 °C in a 0.5 M $NaHCO_3$ solution purged with CO_2, 1 atm, pH 7.5.

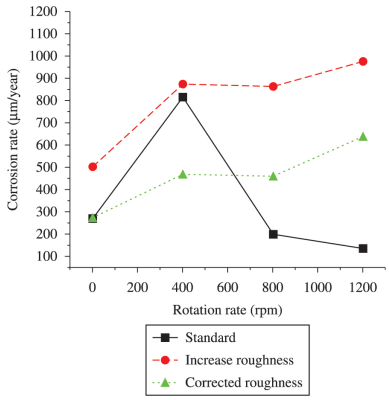

Figure 6. CO_2 Corrosion rates obtained by lpr method at four rotation rates: 0, 400, 800 and 1200 RPM from each superficial finish conditions: standard, increased roughness (blasted) and corrected roughness. of AISI 1020 steel at 25 °C in a 0.5 M $NaHCO_3$ solution purged with CO_2, 1 atm, pH 7.5.

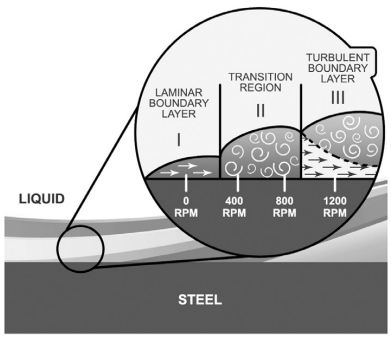

Figure 7. Schematic regions in the velocity boundary layer associated with electrode rotation velocity.

The area factor, F = 1.880 (Equation 12), of the cylinder surface with the increased roughness, was considered in the Stern-Geary equation and the new corrosion rate was obtained, this corrosion rate was represented by corrected roughness curve. The CO_2 corrosion rate value shows a clear dependence on the rotation rate and superficial finish conditions. This can be explained mainly by the action of the viscous forces on the liquid mass, originating both from the quality of the interaction between the species present in the fluid (velocity) and from the fluid/electrode border effect (roughness).

When the electrode rotation increases, causing an increase in its superficial velocity in order to reach a turbulent flow regime, two different regions appear: one next to the cylinder wall and another involving the remaining fluid. In the region adjacent to the metal/fluid border, called the hydrodynamic boundary layer, the fluid molecules in contact with the metallic surface adhere to the surface and cause a stagnation effect in the solution, which develops a velocity gradient.

In the laminar boundary layer condition, the dissolution mechanism of the Fe^{2+} species increases according to the velocity, until it reaches a transition region. The experimental results obtained showed that the type of interaction on the electrode surface with the fluid is modified for velocities near 400 rpm, and is displaced to the laminar boundary layer (region I) to the right (region II) as shown in Figure 7. The hydrodynamics on the cylinder electrode surface is considered uniform for each rotation condition. This means that with the increase in cylinder rotation the hydrodynamic condition on the electrode surface changes from static behavior to laminar behavior to one corresponding to the transition regime until it reaches the totally turbulent flow in which the laminar underlayer is formed.

In the transition region, region II in Figure 7, the Fe^{2+} and CO_3^{2-} species begin to experience the rotation movement (micro vortices) that makes solution saturation difficult and increases the pH between the $FeCO_3$ layer pores, resulting in a corrosion rate peak.

When the electrode velocity is increased even more, the boundary layer is displaced to the turbulent condition (region III), developing an underlayer called laminar underlayer (see Figure 7). In the laminar underlayer, the viscous effects are important and allow not only the formation of a protective layer, but also its positioning on the electrode surface, a pH increase and solution saturation between the pores, progressively reducing the corrosion rate since the underlayer thickness reduces with the increased flow and there is formation of Fe_3O_4 in the pores of the iron carbonate layer.

When the laminar underlayer condition is reached in surfaces with less roughness, the corrosion processes are similar to the condition of the fluid at rest. The corrosion rate decrease due to the increase in the diffusion gradient of the reactive species since the underlayer thickness is quite reduced, which favors solution saturation between the pores.

When the friction factor of the cylinder surface with the increased roughness was taken into consideration, the experimental results showed that roughness facilitates the precipitation mechanism of the $FeCO_3$ layer and increases the shear stress of the fluid. When the cylinder velocity and the shear stress of the fluid are increased, the fluid interaction with the surface quickly goes from a laminar regime to the transition region. The superficial irregularities in the transition region permit the formation of micro vortices and this phenomenon progressively increases the steel corrosion rate as shown in Figure 6. Thus, the increase in superficial roughness causes an increase in the corrosion rate without allowing the electrode surface to experience the laminar underlayer condition. It follows that the corrosion rate remains high for the velocity flow range evaluated.

4. Conclusions

The behavior described in this paper indicates the influence of the laminar/turbulent flow transition zone on dissolution kinetics and on the formation of the iron carbonate layer. The maximum CO_2 corrosion rate value obtained for the smoother electrode occurs when the structure of the hydrodynamic boundary layer is between the turbulent and laminar regions and may be associated with this transition region in which micro vortices and, consequently, high agitation of the species near the surface, are observed and inhibit the $FeCO_3$ layer precipitation process. When surface roughness was considered in the corrosion rate calculations, from the area factor, F, the corrosion rate for corrected roughness, decreased for all rotation rates conditions, due to an increase in area available for the anodic reaction. However, turbulent flow has different effects on standard and rough surface. On the surface roughness, the turbulent eddies enhance the flow-induced corrosion and an increase in rotation rate results in an increase in corrosion rate.

References

1. Dugstad A and Halseid M. *Internal corrosion in dense phase CO2 transport pipelines: state of the art and the need for further R&D*. Houston: NACE International; 2012. Corrosion Paper nº 0001452.
2. Le Crolet J, Thevenot N and Nesic S. Role of conductive corrosion products in the protectiveness of corrosion layers. *Corrosion*. 1998; 54(3):194-203. http://dx.doi.org/10.5006/1.3284844.
3. Le Crolet J and Bonis MR. pH measurement in aqueous co2 solutions under high pressure and temperature. *Corrosion*. 1983; 39(2):39-46. http://dx.doi.org/10.5006/1.3580813.
4. Nesic S, Shihuai W, Cai J and Xiao Y. *Integrated CO2 corrosion: multiphase flow model*. Houston: NACE International. Corrosion Paper nº 04626.
5. Han J, Young D and Nesic S. *Characterization of the passive film on mild steel in CO2 environments*. Houston: NACE International. Corrosion Paper nº 2511.
6. Hassani SH, Roberts KP, Shirazi SA, Shadley JR, Rybicki EF and Joia C. Flow loop study of NaCl concentration effect on erosion, corrosion and erosion-corrosion of carbon steel in CO2-satured systems. *Corrosion*. 2012; 68(2):026001-1-026001-9. http://dx.doi.org/10.5006/1.3683229.
7. Ferreira LRM. *Avaliação da corrosão por fluxo do aço AISI 1020 em solução de NaHCO3 saturada de CO2*. [Dissertation]. Curitiba: Parana Federal University; 2012.
8. Shayegani M, Ghorbani M, Afshar A and Rahmaniyan M. Modelling of carbon dioxide corrosion of steel with iron carbonate precipitation. *Corrosion Engineering, Science and Technology*. 2009; 44(2):128-136. http://dx.doi.org/10.1179/174327808X286338.
9. Nesic S, Postlethwaite J and Olsen S. An Electrochemical Model for Prediction of Corrosion of Mild Steel in Aqueous Carbon Dioxide Solution. *Corrosion*. 1996; 52(4):280-294. http://dx.doi.org/10.5006/1.3293640.
10. Han J, Young D and Nesic S. *Characterization of the passive film on mild steel in CO2 environments*. Houston: NACE International; 2009. Corrosion Paper nº 2511.
11. Asma RBA, Yuli PA and Mokhtar CI. Study on the effect of surface finish on corrosion of carbon steel in CO2 environment. *Journal of Applied Sciences*. 2011; 11(11):2053-2057. http://dx.doi.org/10.3923/jas.2011.2053.2057.
12. Fox RW. *Introduction to fluid mechanics*. 4th ed. John Wiley & Sons; 1992.
13. Silverman DC and Winston R. Pratical corrosion prediction using electrochemical techniques. In: Winston Revie R, editor. *Uhlig's Corrosion Handbook*. 3th ed. Hoboken: John Wiley & Sons; 2011.
14. American Society for Testing and Materials - ASTM. *ASTM G185-06: standard practice for evaluating and qualifying oil field and refinery corrosion inhibitors the rotating cylinder electrode*. West Conshohocken.
15. Welty JR, Wicks CE, Wilson RE and Rorrer G. *Fundamentals of momentum, heat and mass transfer*. 4th ed. John Wiley & Sons; 2001.